J Solid State Electrochem (2001) 5: 459–465
DOI 10.1007/s100080100198

ORIGINAL PAPER

Jong-Won Lee · Jeong-Nam Han · Masahiro Seo
Su-Il Pyun

Transport of alkaline cation and neutral species through the α-Ni(OH)$_2$/γ-NiOOH film electrode

Received: 3 September 2000 / Accepted: 18 January 2001 / Published online: 7 June 2001

Abstract The transport of alkaline cation and neutral species through the α-Ni(OH)$_2$/γ-NiOOH film electrode has been investigated during the hydrogen extraction from and injection into the film electrode in 0.1 M LiOH, KOH and CsOH solutions by using the electrochemical quartz crystal microbalance technique combined with the potentiostatic current transient technique and cyclic voltammetry. From the ohmic relationship between the initial current density and the applied potential step, it is suggested that the hydrogen transport through the film electrode is exclusively governed by "cell-impedance". On the basis of the "cell-impedance-controlled" hydrogen transport, the mass change measured indicates that during the hydrogen extraction, the alkaline cation is slowly inserted into the film electrode before the finish of the current plateau. After the period of current plateau has finished, it is drastically inserted at an exponential rate. By contrast, during the hydrogen injection, the extraction of alkaline cation is nearly completed before the finish of the current plateau. Most of the neutral species are incorporated into the film electrode during the immersion prior to the hydrogen extraction. The minority is not incorporated until the finish of the current plateau during the hydrogen injection.

Presented at the international conference "Solid State Chemistry 2000", 3–8 September 2000, Prague, Czech Republic

J.-W. Lee · J.-N. Han · S.-I. Pyun (✉)
Department of Materials Science and Engineering,
Korea Advanced Institute of Science and Technology,
373-1 Kusong-Dong, Yusong-Gu,
Taejon 305-701, Korea
E-mail: sipyun@mail.kaist.ac.kr
Tel.: +82-42-8693319
Fax: +82-42-8693310

M. Seo
Graduate School of Engineering,
Hokkaido University, N13W8, Kita-Ku,
Sapporo 060-8628, Japan

Keywords Ni(OH)$_2$/NiOOH film electrode · Electrochemical quartz crystal microbalance · Hydrogen transport · Alkaline cation · Neutral species

Introduction

For several decades, hydrogen transport through the Ni(OH)$_2$/NiOOH electrode has been extensively investigated because of its application in electrochromic devices and secondary batteries [1, 2, 3, 4, 5, 6, 7, 8]. It has been reported from the observation of the colour boundary motion [3] that the hydrogen transport through the Ni(OH)$_2$/NiOOH electrode proceeds via the phase boundary movement in a thickness direction. On the other hand, it has been proposed [2, 4, 7] that the hydrogen transport is controlled by the hydrogen diffusion in the homogeneous phase, not by the phase boundary movement. It is still open to question what mechanism is appropriate for the hydrogen transport through the Ni(OH)$_2$/NiOOH electrode.

It is generally known [9] that the Ni(OH)$_2$/NiOOH electrode is classified into two distinct systems of α-Ni(OH)$_2$/γ-NiOOH and β-Ni(OH)$_2$/β-NiOOH. In battery applications, the former electrode has superior electrochemical properties compared with the latter electrode [10, 11, 12]; however, the electrochemical process of the former electrode is more complicated owing to the two following reasons: one is that the γ-NiOOH has a complex structure with a nickel valency higher than 3 [10, 13, 14, 15] and the other is that the hydrogen transport through the α-Ni(OH)$_2$/γ-NiOOH electrode is accompanied by the transport of alkaline cation and neutral species [12, 16, 17, 18, 19].

In particular, many researchers [12, 16, 17, 18, 19] have explored the transport of alkaline cation and neutral species through the α-Ni(OH)$_2$/γ-NiOOH electrode from the analysis of mass change obtained during cyclic voltammetric measurement; however, they gave simply the direction of the transport of alkaline cation and neutral

species during the hydrogen extraction from and injection into the α-$Ni(OH)_2$/γ-NiOOH electrode. It is necessary to investigate further the kinetics of the transport of alkaline cation and neutral species coupled with the hydrogen transport through the α-$Ni(OH)_2$/γ-NiOOH electrode; therefore, the present work aims, first, at clarifying the mechanism of the hydrogen transport and, second, at exploring the kinetics of the transport of alkaline cation and neutral species through the α-$Ni(OH)_2$/γ-NiOOH film electrode. For this purpose the anodic and cathodic current transients were measured on the film electrode in 0.1 M LiOH, KOH and CsOH solutions and analysed. In parallel, the mass change simultaneously measured with the current transient and cyclic voltammogram was analysed in the same electrolyte on the basis of the hydrogen-transport mechanism suggested in this work.

Experimental

The $Ni(OH)_2$ film specimen was deposited galvanostatically on the gold-coated side of a quartz crystal with a constant current density of 0.1 mA cm^{-2} for 10 min in 0.1 M $Ni(NO_3)_2$ solution. The mass of the electrodeposited $Ni(OH)_2$ film was measured to be 38.86 μg cm^{-2} using an electrochemical quartz crystal microbalance (EQCM) (Seiko EG&G QCA 917). The gold was previously sputtered to a thickness of 0.3 μm and 0.2 cm^2 in area onto both sides of the 9 MHz AT-cut quartz crystal in a keyhole pattern by the manufacturer (Seiko EG&G). From the X-ray diffraction pattern, we confirmed that the $Ni(OH)_2$ film electrode electrodeposited in this work is composed of an α modification with disordered turbostratic structure.

A platinum wire and a mercury/mercury oxide electrode were used as a counter electrode and a reference electrode, respectively. The electrolytes involved were 0.1 M LiOH, KOH and CsOH solutions and were deaerated for 24 h by bubbling through them purified argon gas, which contains 1.0 ppm O_2, 8.0 ppm N_2 and 1.0 ppm H_2O by weight, before all the electrochemical experiments.

The freshly deposited film was previously rinsed with distilled water and then immersed in the electrolyte for 30 min. After that, the $Ni(OH)_2$ film electrode was first polarised at a potential of 0.25 $V_{Hg/HgO}$ for 10 min, followed by jumping the potential to 0.55 $V_{Hg/HgO}$ using an EG&G PARC model 263A potentiostat. After keeping the film electrode at this potential for 10 min, the potential was dropped to 0.25 $V_{Hg/HgO}$. From the moment of the potential jump and drop on, the resulting anodic current and cathodic current were consecutively recorded with time during the hydrogen extraction and injection, respectively. The hydrogen extraction and injection are sometimes termed the proton extraction and injection, respectively, in the literature.

Cyclic voltammetry was performed on the film electrode in the potential range 0.2–0.6 $V_{Hg/HgO}$ with a scan rate of 1 mV s^{-1} by employing an EG&G PARC model 263A potentiostat.

The mass change was simultaneously measured on the film electrode with the current transient and cyclic voltammogram by using the EQCM. All the experiments were conducted at ambient temperature.

Results and discussion

The anodic and cathodic current transients on a logarithmic scale, log$i$ versus log$t$, measured on the α-$Ni(OH)_2$/γ-NiOOH film electrode in 0.1 M LiOH, KOH and CsOH solutions during the hydrogen extraction by jumping a potential of 0.25 to 0.55 $V_{Hg/HgO}$ and during the hydrogen injection by dropping a potential of 0.55 to 0.25 $V_{Hg/HgO}$ are shown in Fig. 1a and b, respectively.

The anodic and cathodic current transients exhibit the three-stage shape, composed of a current plateau, then a sudden fall of current with time, followed by a concave downward curve. The three-stage current transient including the current plateau was also observed in

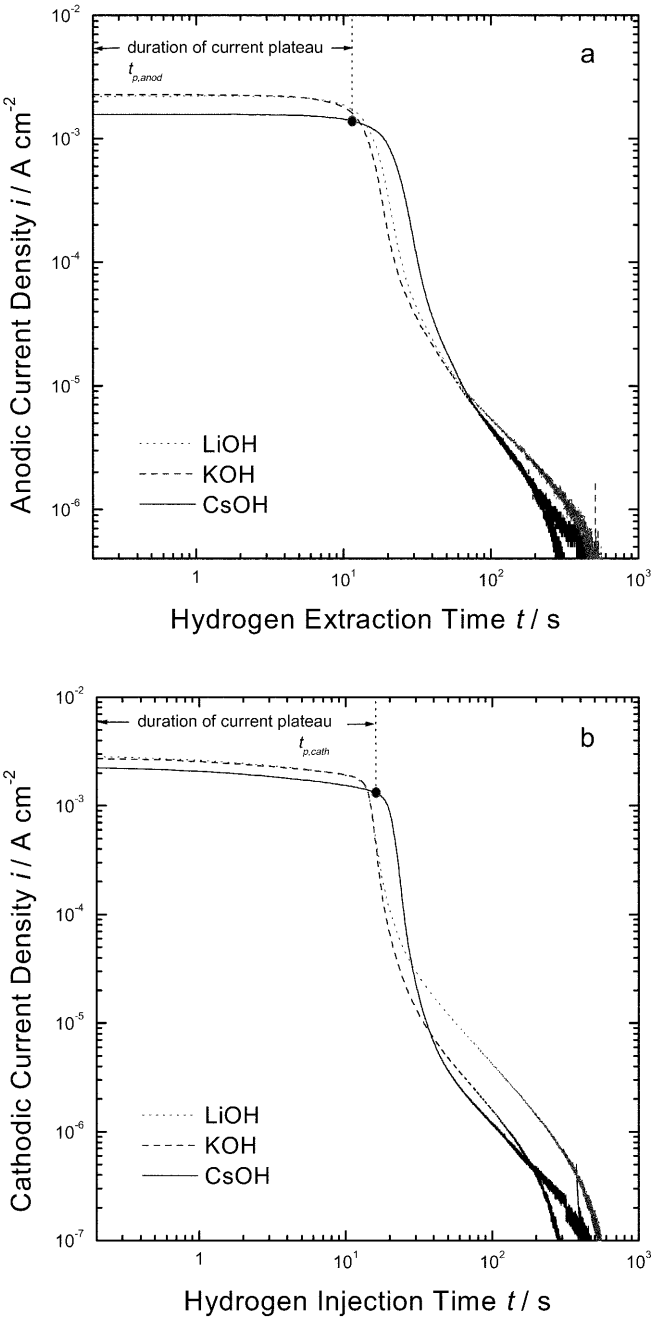

Fig. 1 **a** The anodic current transients during the hydrogen extraction by jumping a potential of 0.25 to 0.55 $V_{Hg/HgO}$ and **b** the cathodic current transients during the hydrogen injection by dropping a potential of 0.55 to 0.25 $V_{Hg/HgO}$, on a logarithmic scale, log$i$ versus log$t$, measured on the α-$Ni(OH)_2$/γ-NiOOH film electrode in 0.1 M LiOH, KOH and CsOH solutions

previous work [8]. All the anodic and cathodic current transients measured in LiOH, KOH and CsOH solutions have the same shape; however, the heights of the current plateaux, i_p, obtained from the anodic and cathodic current transients in CsOH solution are smaller by about 1 mA cm^{-2} than those values obtained from the anodic and cathodic current transients in LiOH and KOH solutions.

The durations of the current plateaux, $t_{p,anod}$, during the hydrogen extraction were measured to be approximately 9 s in LiOH solution, 9 s in KOH solution and 12 s in CsOH solution. The lengths of current plateau period, $t_{p,cath}$, measured as a function of electrolyte during the hydrogen injection are almost the same as those values determined during the hydrogen extraction. It is worthwhile noting that the length of t_p in CsOH solution is markedly greater than the values in LiOH and KOH solutions. The amount of hydrogen extracted from and injected into the film electrode during t_p was calculated by integrating the anodic current transients in Fig. 1a and the cathodic current transients in Fig. 1b with respect to time up to t_p, which yields about 75% of the total amount of hydrogen extracted and injected, regardless of the kind of electrolyte.

By taking the total charge transferred during the hydrogen extraction in 0.1 M KOH solution, Q, the hydrogen diffusivity, D_H, and the film thickness, L, as 3.2×10^{-2} C cm^{-2} measured from Fig. 1a, 6.4×10^{-11} cm^2 s^{-1} [7] and 0.11 μm, respectively, we calculated the value of the initial anodic current density, $i_{ini,anod}$, at 0.2 s from the Cottrell equation for the short time region [20]. The calculation of $i_{ini,anod}$ gave 2.9×10^{-2} A cm^{-2}, which is larger in value by about 1 order of magnitude than that value of $i_{ini,anod}$ measured experimentally (2.3×10^{-3} A cm^{-2}). The values of i_{ini} calculated are larger in value by about 1 order of magnitude than the values of i_{ini} measured in the other alkaline solutions, as well.

$i_{ini,anod}$ observed at 0.2 s from the anodic current transient of Fig. 1a is plotted in Fig. 2a against the anodic potential jump ΔE_{jump}, at the initial potential of 0.25 $V_{Hg/HgO}$. $i_{ini,anod}$ is linearly proportional to ΔE_{jump}, viz. the initial current density–potential relation follows Ohm's law. In addition, during the hydrogen injection the linear relationship is also satisfied between the initial cathodic current density, $i_{ini,cath}$, and the cathodic potential drop, ΔE_{drop}, at the initial potential of 0.55 $V_{Hg/HgO}$, which is given in Fig. 2b.

Recently, Shin and coworkers [21, 22, 23] observed the linear relationship between the initial current level and the applied potential step during the lithium intercalation into and the lithium deintercalation from transition-metal oxides such as $Li_{1-\delta}CoO_2$, $Li_{1+\delta}(Ti_{5/3}Li_{1/3})O_4$, $Li_{1-\delta}NiO_2$ and $Li_\delta V_2O_5$ and concluded that in this case the lithium transport through the electrode is purely governed by "cell-impedance".

Consequently, from the previous results that the initial current density measured experimentally is much smaller than the calculated initial current density under the "diffusion-controlled" constraint and from the fact that the initial current density–potential relation obeys Ohm's law, it is suggested that the gradient of the hydrogen concentration at the electrode surface is given by the quotient of the applied potential step, ΔE, divided by the "cell-impedance", R_{cell}. In other words, the hydrogen transport through the α-$Ni(OH)_2/\gamma$-NiOOH film

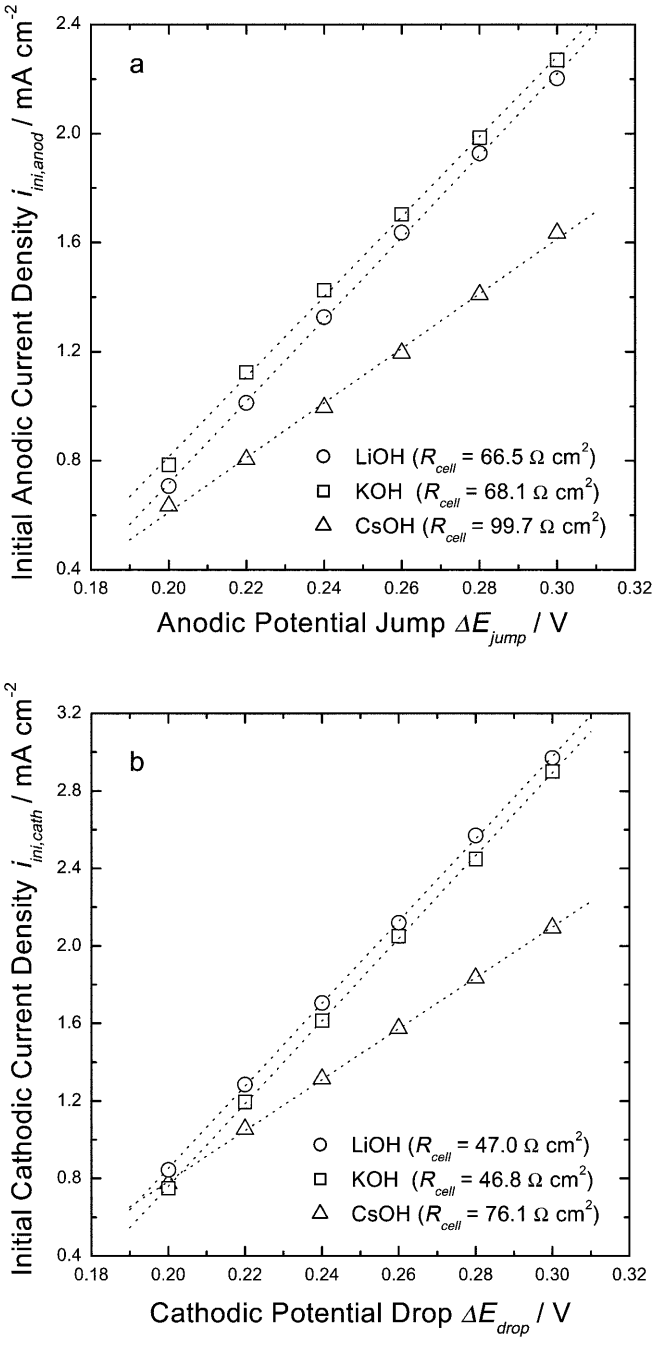

Fig. 2 Plot of **a** initial anodic current density, $i_{ini,anod}$, against anodic potential jump, ΔE_{jump}, at 0.25 $V_{Hg/HgO}$ and **b** initial cathodic current density, $i_{ini,cath}$, against cathodic potential drop, ΔE_{drop}, at 0.55 $V_{Hg/HgO}$. $i_{ini,anod}$ and $i_{ini,cath}$ were obtained 0.2 s from the anodic current transients of Fig. 1a and the cathodic current transients of Fig. 1b, respectively

electrode proceeds under the "cell-impedance-controlled" constraint.

In previous work [8], the current plateau observed in the current transient was analysed on the basis of the phase boundary movement. As a consequence, it was suggested that the current plateau is attributed to the interface-controlled phase boundary movement; however, from the linear relationship between the initial current density and the applied potential step obtained in the present work, it is indicated that the hydrogen transport through the film electrode proceeds under the "cell-impedance-controlled" constraint, not by the phase boundary movement.

The values of R_{cell} at the initial potentials of 0.25 and 0.55 $V_{Hg/HgO}$ calculated from the slope of the i_{ini} versus ΔE plot are presented in Fig. 2a and b, respectively. It should be emphasised that the values of R_{cell} in LiOH and KOH solutions almost coincide, but they are much smaller than the value in CsOH solution. Considering that R_{cell} determines the current transient in value and shape, it is reasonable to consider that the fall in the height of i_p and the extension of t_p in CsOH solution in Fig. 1 are ascribed to the rise in R_{cell} in CsOH solution determined in Fig. 2.

The changes in the mass of the film electrode, Δm_f, measured during the immersion in 0.1 M LiOH, KOH and CsOH solutions for 30 min prior to the hydrogen extraction are demonstrated in Fig. 3. Δm_f increases to a constant value of about 1.35 μg cm^{-2} with progressing immersion time, irrespective of the kind of electrolyte. This indicates that certain common species contained in the three kinds of electrolyte are incorporated into the film electrode during the immersion. Thus, the species

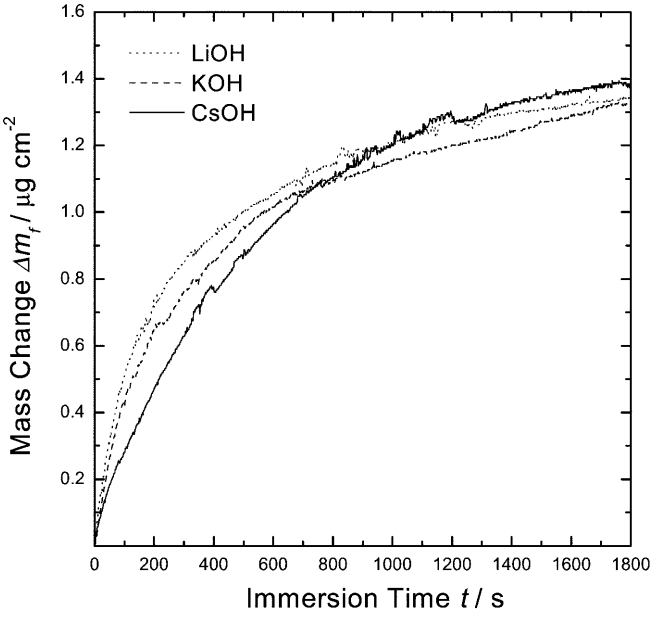

Fig. 3 Plot of the mass change, Δm_f, in the α-$Ni(OH)_2$/γ-NiOOH film electrode versus immersion time, t, measured in 0.1 M LiOH, KOH and CsOH solutions for 30 min prior to the hydrogen extraction

incorporated are expected to be water molecules, not alkaline cations and salts such as LiOH, KOH and CsOH molecules [19].

It is known [24, 25] that anions such as NO_3^- or CO_3^{2-} in the electrolyte are intercalated into the film electrode during the electrodeposition of $Ni(OH)_2$ film and expand the interlayer space between NiO_2 slabs producing the structure of α-$Ni(OH)_2$. Considering that water molecules are incorporated into the film electrode during the immersion stage preceded by the electrodeposition, it is inferred that the remaining free interlayer space caused by the anion intercalation is occupied by water molecules and, as a consequence, the incorporation of water molecules stabilizes the expanded interlayer space.

Figure 4a and b displays the mass change transients on a semilogarithmic scale, Δm_f versus log$t$, measured simultaneously with the anodic and cathodic current transients in Fig. 1a and b, respectively, on the film electrode in 0.1 M LiOH, KOH and CsOH solutions. t_p in Fig. 1 are also designated in Fig. 4.

Figure 4a shows that as the hydrogen extraction progresses to the finish of the current plateau $t_{p,anod}$, m_f falls to a minimum in LiOH solution, it remains constant in KOH solution and it slowly increases in CsOH solution. With further hydrogen extraction, m_f rapidly increases to a saturated value in all three kinds of electrolyte. The heavier the alkaline cation, the more markedly m_f increases.

From the analysis of the mass change measured with the EQCM, it is reported [12, 16, 17, 18] that the oxidation reaction of the α-$Ni(OH)_2$ phase involves the hydrogen extraction and the insertion of alkaline cations such as Li^+, K^+ and Cs^+ ions. As a result, the mass increase during the hydrogen extraction is traced back to the insertion of alkaline cation into the film electrode.

According to the "cell-impedance-controlled" hydrogen transport, the electrode surface is fully covered with the NiOOH phase just after the finish of the current plateau in the anodic current transient. The mass change transient measured simultaneously with the anodic current transient indicates that the insertion rate of the alkaline cation is drastically increased just after the finish of the current plateau. From the analysis of the anodic current transient and the mass change transient, it is suggested that the insertion rate of the alkaline cation is closely associated with the surface coverage by the NiOOH phase.

In this respect, it is conceivable that more alkaline cation is inserted into the film electrode as coverage of the electrode surface increases to unity by the NiOOH phase until the finish of the current plateau $t_{p,anod}$. Thus, during $t_{p,anod}$ the mass diminution due to the hydrogen extraction is not exceeded, is counterbalanced or is exceeded by the mass increase due to the insertion of the alkaline cation, depending upon the mass of the alkaline cation. As a matter of fact, it is seen from Fig. 4a that during $t_{p,anod}$ the mass decrease by the hydrogen extraction in LiOH solution is dominant over the mass

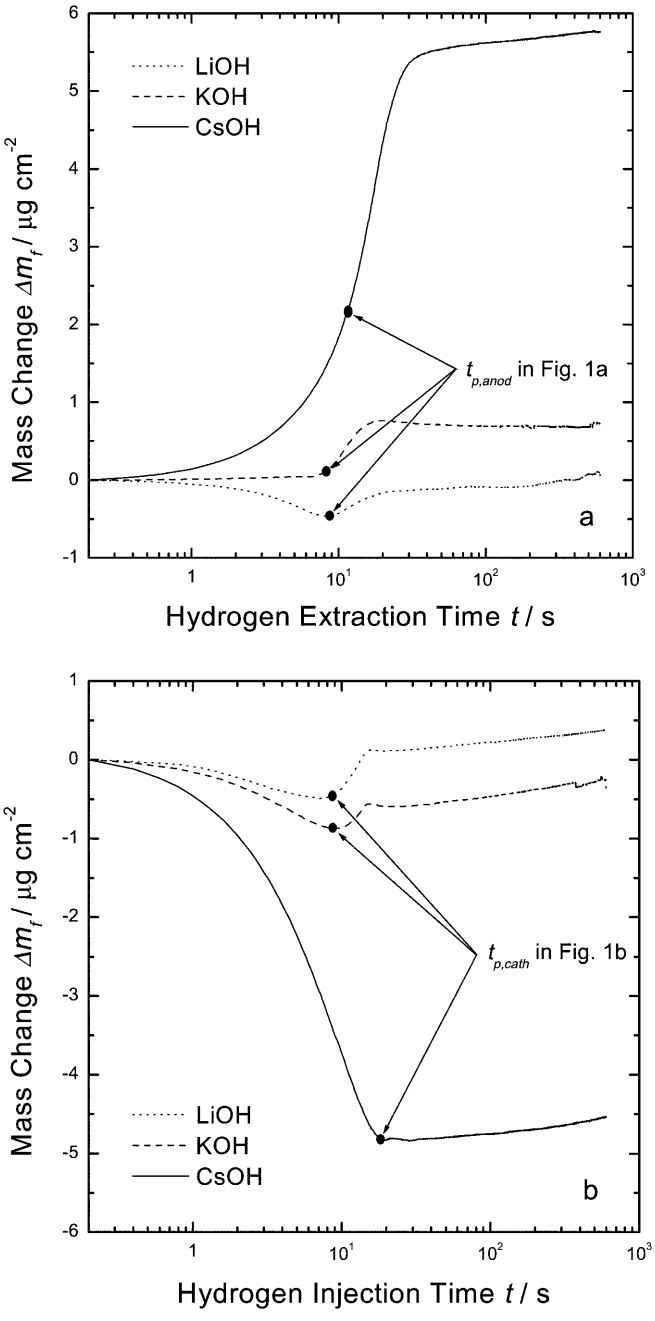

Fig. 4 **a** The mass change transients measured simultaneously with the anodic current transients of Fig. 1a and **b** the mass change transients measured simultaneously with the cathodic current transients of Fig. 1b, on a semilogarithmic scale, Δm_f versus log$t$

increase by the insertion of the alkaline cation, whereas the opposite is valid for CsOH solution.

Since the degree of coverage by the NiOOH phase goes to unity for $t > t_{p,anod}$, the alkaline cation is drastically inserted into the film electrode after $t_{p,anod}$. Considering that the hydrogen extraction is already completed to 75% before the finish of $t_{p,anod}$, the insertion of the alkaline cation contributes mostly to the mass gain. From Fig. 4a, it is seen that the limit of the final mass gain increases in the order of Li^+-, K^+- and Cs^+-containing electrolytic solutions.

Figure 4b shows that as the hydrogen injection runs to the finish of $t_{p,cath}$, m_f decreases to a minimum in LiOH, KOH and CsOH solutions. The heavier the alkaline cation, the more m_f diminishes. With further hydrogen injection, m_f increases to its saturated value in LiOH and KOH solutions, but it remains constant in CsOH solution.

By contrast, as coverage of the electrode surface by the NiOOH phase decreases from unity until the finish of $t_{p,cath}$, the alkaline cation is mostly extracted from the film electrode. At the same time, the hydrogen injection is already completed to 75% before the finish of $t_{p,cath}$. Thus, it is readily seen from Fig. 4b that during $t_{p,cath}$ the mass increase due to the hydrogen injection is much exceeded by the mass diminution due to the extraction of the alkaline cation in all three kinds of electrolyte. Since the degree of coverage by the NiOOH phase approaches zero for $t > t_{p,cath}$, the alkaline cation is hardly extracted from the film electrode after $t_{p,cath}$.

Let us discuss the increase in m_f after the finish of $t_{p,cath}$. Taking into account that only 25% of the total hydrogen transferred is to be injected into the film electrode after $t_{p,cath}$, it is plausible that the increase in m_f after $t_{p,cath}$ ensues mostly from the incorporation of another species into the film electrode rather than from the hydrogen injection. Recently, it was reported [19] that neutral species such as water molecules can be incorporated into the α-Ni(OH)$_2$/γ-NiOOH electrode during the hydrogen injection. In this respect, it is reasonable to accept that such an increase is attributed to the incorporation of water molecules. However, the rise of m_f in CsOH solution does not appear after $t_{p,cath}$. Bearing in mind that the mass of the Cs^+ ion is about 7.5 times larger than that of a water molecule, it seems that the mass increase due to the incorporation of water molecules is cancelled by the mass decrease due to the extraction of the Cs^+ ion.

The cyclic voltammograms and cyclic voltamassograms measured simultaneously on the film electrode in 0.1 M LiOH, KOH and CsOH solutions with a scan rate of 1 mV s^{-1} are illustrated in Fig. 5a and b, respectively. During the scanning of the applied potential from 0.2 to 0.6 $V_{Hg/HgO}$ in the anodic direction, an anodic current peak due to the hydrogen extraction appears in the range 0.4–0.55 $V_{Hg/HgO}$, followed by the oxygen evolution above 0.55 $V_{Hg/HgO}$. The anodic current peak in CsOH solution shifts in the anodic direction and is broader compared with those in LiOH and KOH solutions. At the same time, m_f increases to a saturated value. The limit of the final mass gain increases in the sequence of Li^+-, K^+- and Cs^+-containing electrolytic solutions, which is in good agreement with the result presented in Fig. 4a.

In similar way, during the scanning of the applied potential in the reverse direction, a cathodic current peak corresponding to the hydrogen injection emerges in the range 0.4–0.25 $V_{Hg/HgO}$. In this range, m_f returns to the initial value, regardless of the kind of electrolyte.

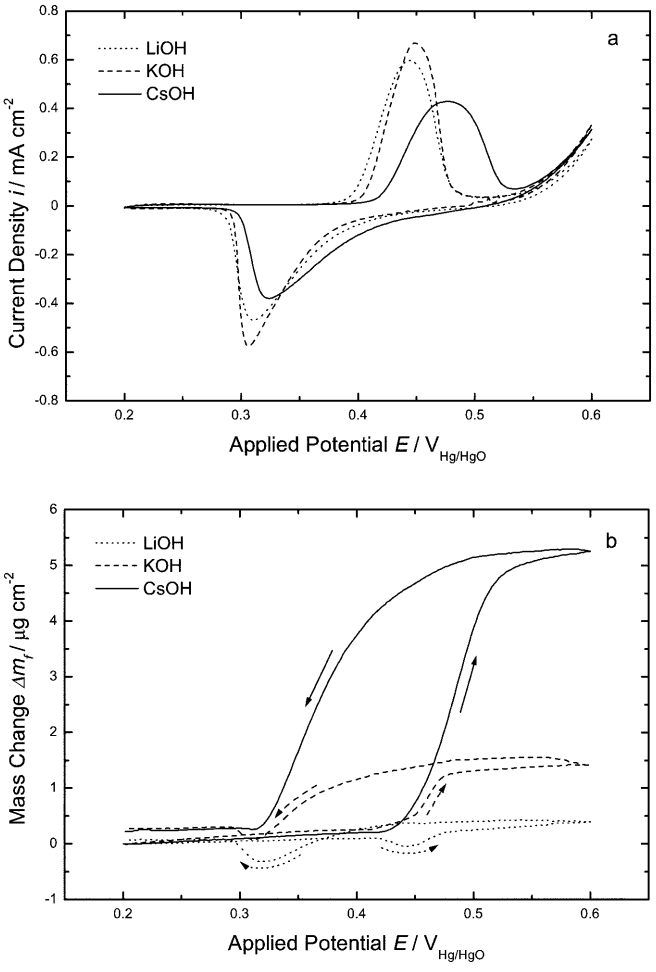

Fig. 5 **a** Cyclic voltammograms and **b** cyclic voltamassograms, measured simultaneously on the α-$Ni(OH)_2/\gamma$-NiOOH film electrode in 0.1 M LiOH, KOH and CsOH solutions with a scan rate of 1 mV s^{-1}

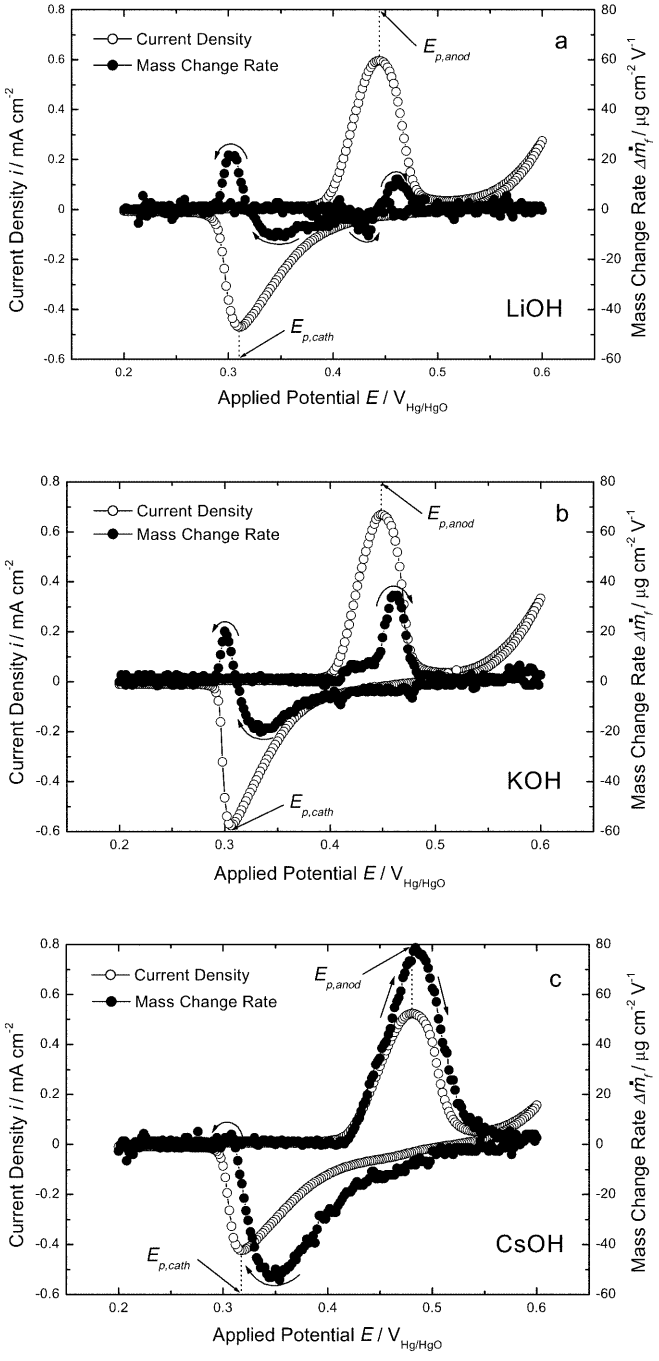

Fig. 6 Cyclic voltammogram and mass change rate curve, measured simultaneously on the α-$Ni(OH)_2/\gamma$-NiOOH film electrode in **a** 0.1 M LiOH, **b** 0.1 M KOH and **c** 0.1 M CsOH solutions with a scan rate of 1 mV s^{-1}

In order to compare the cyclic voltamassogram directly with the cyclic voltammogram, it is convenient to convert the Δm_f into the mass change rate $\Delta \dot{m}_f$. The mass change rate curve was obtained by differentiating the cyclic voltamassogram given in Fig. 5b with respect to the applied potential. The mass change rate curves are given in Fig. 6a, b and c along with the cyclic voltammograms in 0.1 M LiOH, KOH and CsOH solutions, respectively.

At the potential corresponding to the anodic current peak, $E_{p,anod}$, the mass change rate in LiOH solution exhibits a transition from a negative to a positive value and this curve in KOH solution has a transition in positive slope from a low to a high value. However, this curve in CsOH solution exhibits no transition of the positive slope over the wide potential range of the anodic current peak.

In LiOH solution (Fig. 6a), the negative value of the mass change rate below $E_{p,anod}$ indicates that the mass diminution due to the hydrogen extraction dominates over the mass increase due to the Li^+ ion insertion. This is analogous to the case of $t < t_{p,anod}$, obtained from Fig. 4a. By contrast, the positive value of the mass change rate above $E_{p,anod}$ reveals that the mass gain by the Li^+ ion insertion dominates over the mass loss by the hydrogen extraction. This is similar to the case for $t > t_{p,anod}$ obtained from Fig. 4a. In similar way, the slight rise in the mass change rate curve of Fig. 6b below $E_{p,anod}$ followed by the sharp rise above $E_{p,anod}$ in KOH

solution means that the mass gain by the K^+ ion insertion is somewhat dominant below $E_{p,anod}$ and then becomes more dominant above $E_{p,anod}$. However, the mass loss by the hydrogen extraction in CsOH solution is negligibly small compared with the mass gain by the Cs^+ ion insertion, which contributes mostly to the mass increase through the wide potential range of the anodic current peak. This is analogous to the case of $t \leq t_{p,anod}$ and $t > t_{p,anod}$ obtained from Fig. 4a.

At the potential corresponding to the cathodic current peak, $E_{p,cath}$, all the mass change rates in LiOH, KOH and CsOH solutions exhibit a transition from a negative to a positive value. This means that the alkaline cation is mostly extracted from the film electrode above $E_{p,cath}$, but neutral species such as water molecules are incorporated into the film electrode below $E_{p,cath}$. The mass loss by the extraction of alkaline cation above $E_{p,cath}$ is analogous to that mass loss before the finish of $t_{p,cath}$ in Fig. 4b. Similarly, the mass gain by the incorporation of neutral species below $E_{p,cath}$ is similar to that mass gain after the finish of $t_{p,cath}$ in Fig. 4b.

Conclusions

The present work considers the transport of alkaline cation and neutral species through the α-$Ni(OH)_2$/γ-NiOOH film electrode during the hydrogen extraction from and injection into the film electrode in 0.1 M LiOH, KOH and CsOH solutions by employing the EQCM technique supplemented by the potentiostatic current transient technique and cyclic voltammetry.

1. The mass change obtained during the immersion prior to the hydrogen extraction indicates that the incorporation of neutral species such as water molecules proceeds mainly during the immersion. The remaining minor amount of neutral species is not incorporated into the film electrode until the finish of the current plateau during the hydrogen injection, preceded by the hydrogen extraction.
2. From the linear relationship between the initial current density and the applied potential step, it is concluded that the hydrogen output/input flux at the electrode surface is given by the quotient of applied potential step divided by the ''cell-impedance''. This means that the hydrogen transport is purely controlled by ''cell-impedance''.
3. From the analysis of the mass change measured simultaneously with the current transient and the cyclic voltammogram, the alkaline cation movement in the film electrode is summarised as follows. During the hydrogen extraction, the alkaline cation is slowly inserted into the film electrode before the finish of the current plateau. After the period of the current plateau has finished, it is inserted abruptly. In contrast, during the hydrogen injection, the extraction of the alkaline cation is almost complete before the finish of the current plateau.

Acknowledgements The present work was carried out under the auspices of the joint program of the Korea Science and Engineering Foundation (KOSEF) and the Japan Society for the Promotion of Science (JSPS) 1999/2001. The authors are indebted to the KOSEF for the financial support of this work. Furthermore, this work was partly supported by the Brain Korea 21 project.

References

1. MacArthur DM (1970) J Electrochem Soc 117:422
2. MacArthur DM (1970) J Electrochem Soc 117:729
3. Briggs GWD, Fleischmann M (1971) Trans Faraday Soc 67:2397
4. Briggs GWD, Snodin PR (1982) Electrochim Acta 27:565
5. Zhang C, Park S-M (1987) J Electrochem Soc 134:2966
6. Huggins RA, Prinz H, Wohlfahrt-Mehrens M, Jörissen L, Witschel W (1994) Solid State Ionics 70–71:417
7. Motupally S, Streinz CC, Weidner JW (1995) J Electrochem Soc 142:1401
8. Yoon Y-G, Pyun S-I (1997) Electrochim Acta 42:2465
9. Bode H, Dehmelt K, Witte J (1966) Electrochim Acta 11:1079
10. Oliva P, Leonardi J, Laurent JF, Delmas C, Braconnier JJ, Figlarz M, Fievet F, de Guibert A (1982) J Power Sources 8:229
11. Kamath PV, Dixit M, Indira L, Shukla AK, Kumar VG, Munichandraiah N (1994) J Electrochem Soc 141:2956
12. Kim M-S, Hwang T-S, Kim K-B (1997) J Electrochem Soc 144:1537
13. Tuomi D (1965) J Electrochem Soc 112:1
14. Barnard R, Randell CF, Tye FL (1980) J Appl Electrochem 10:109
15. Corrigan DA, Knight SL (1989) J Electrochem Soc 136:613
16. Cordoba-Torresi SI, Gabrielli C, Hugot-Le Goff A, Torresi R (1991) J Electrochem Soc 138:1548
17. Faria IC, Torresi R, Gorenstein A (1993) Electrochim Acta 38:2765
18. Cheek GT, O'Grady WE (1997) J Electroanal Chem 421:173
19. Gonsalves M, Hillman AR (1998) J Electroanal Chem 454:183
20. Bard AJ, Faulkner LR (1980) Electrochemical methods. Wiley, New York, p 143
21. Shin H-C, Pyun S-I (1999) Electrochim Acta 45:489
22. Shin H-C, Pyun S-I, Kim S-W, Lee M-H (2000) Electrochim Acta 46:897
23. Lee M-H, Pyun S-I, Shin H-C (2000) Solid State Ionics 140:35
24. Delmas C, Faure C, Borthomieu Y (1992) Mater Sci Eng B 13:89
25. Wohlfahrt-Mehrens M, Oesten R, Huggins RA (1996) Solid State Ionics 86–88:841